Smart Materials and Structures

PAPER

Pop-up assembly of 3D structures actuated by heat shrinkable polymers

To cite this article: Jianxun Cui *et al* 2017 *Smart Mater. Struct.* **26** 125011

View the article online for updates and enhancements.

Related content

- A crawling robot driven by multi-stable origami
  Alexander Pagano, Tongxi Yan, Brian Chien et al.
- Material selection for elastic energy absorption in origami-inspired compliant corrugations
  Sean S Tolman, Isaac L Delimont, Larry L Howell et al.
- Self-folding origami: shape memory composites activated by uniform heating
  Michael T Tolley, Samuel M Felton, Shuhei Miyashita et al.

This content was downloaded from IP address 98.122.160.93 on 09/12/2017 at 22:26

IOP Publishing Smart Materials and Structures
Smart Mater. Struct. **26** (2017) 125011 (9pp) https://doi.org/10.1088/1361-665X/aa9552

Pop-up assembly of 3D structures actuated by heat shrinkable polymers

Jianxun Cui, J G M Adams and Yong Zhu

Department of Mechanical and Aerospace Engineering, North Carolina State University, Raleigh, North Carolina 27695-7910, United States of America

E-mail: yong_zhu@ncsu.edu

Received 22 August 2017, revised 4 October 2017
Accepted for publication 23 October 2017
Published 3 November 2017

Abstract

Folding 2D sheets into desired 3D structures is a promising fabrication technique that can find a wide range of applications. Compressive buckling provides an attractive strategy to actuate the folding and can be applied to a broad range of materials. Here a new and simple method is reported to achieve controlled compressive buckling, which is actuated by a heat shrinkable polymer sheet. The buckling deformation is localized at the pre-defined creases in the 2D sheet, resulting in sharp folding. Two approaches are developed to actuate the transformation, which follow similar geometric rules. In the first approach, the 2D precursor is pushed from outside, which leads to a 3D structure surrounded by the shrunk polymer sheet. Assembled 3D structures include prisms/pyramids with different base shapes, house roof, partial soccer ball, Miura-ori structure and insect wing. In the second approach, the 2D precursor is pulled from inside, which leads to a 3D structure enclosing the shrunk polymer sheet. Prisms/pyramids with different base shapes are assembled. The assembled structures are further tessellated to fabricate cellular structures that can be used as thermal insulator and crash energy absorber. They are also stacked vertically to fabricate complex multilayer structures.

Supplementary material for this article is available online

Keywords: origami, kirigami, controlled buckling, heat shrinkable polymer

(Some figures may appear in colour only in the online journal)

1. Introduction

There is a growing interest in transforming two dimensional (2D) sheets into three dimensional (3D) structures, which can find a wide range of applications including self-folding robots [1–3], deformable batteries [4, 5], containers for drug delivery [6, 7], reconfigurable metamaterials [8–10], and 3D electronic devices [11, 12]. The transformation can be achieved via origami-inspired approaches [11, 13], i.e. folding a 2D sheet along pre-defined creases. Slits or perforations can also be introduced in the 2D sheet prior to folding (known as kirigami), which increases the diversity of accessible 3D shapes [14–18].

In general the 2D-to-3D transformation requires pre-defined crease patterns in the 2D sheet where localized folding occurs and an actuating component [19, 20]. According to the relative location of the actuating component and the creases, two general strategies can be used to realize the transformation. In the first strategy, transformation is actuated by responsive hinges (at the same locations as the creases) [2], which fold when triggered. The responsive hinge can be created by a local bimorph actuator, where folding occurs due to mismatch in thermal expansion [21–24] or swelling [25]. The hinge can also be made directly on the 2D sheet. In this case the 2D sheet is locally modified at the creases, e.g. by light-induced stress relaxation [26] or light-induced heating [27–30], to create a stress gradient across the thickness of the 2D sheet. In the second strategy, the actuating component is away from the creases. For example, an external compressive force can be used to trigger buckling of the 2D sheet, where the buckling is localized at the creases that are more compliant than the rest of the sheet. This strategy does not require responsiveness of the 2D sheet. A number of complex 3D structures have been assembled by controlled

 © 2017 IOP Publishing Ltd Printed in the UK

compressive buckling [31–34]. However, a pre-stretching step was needed in order to apply the compressive force, which is not trivial especially for biaxial stretching and cannot be remotely operated.

In this paper we report a new method to achieve controlled mechanical buckling following the second strategy. Here a heat shrinkable polymer sheet is used to trigger the buckling upon noncontact heating (e.g. in an oven) instead of the pre-stretching. Two approaches are demonstrated. In the first approach, the 2D precursor is inscribed in a perforated pattern (of a specific shape) in the polymer sheet, thus pushed from outside upon heating. After transformation, a 3D structure inscribed in the shrunk perforation is assembled. Several assembled 3D structures are demonstrated including prismatic/pyramidal structures with different base shapes, house roof, partial soccer ball, Miura-ori structure and insect wing. In the second approach, a small piece of polymer sheet with a specific shape is placed on top of the 2D precursor, and pulls it from inside upon heating. After transformation, a 3D structure enclosing the shrunk polymer sheet is formed. Prismatic/pyramidal structures with a variety of base shapes are assembled, which can be tessellated horizontally to create cellular structures and stacked vertically as complex multilayer structures.

2. Experimental section

2.1. Materials

The heat shrinkable polymer sheet, with the brand name of Shrinky-Dinks, was made of pre-strained polystyrene (PS), which shrinks to 46% equi-biaxially (i.e. isotropically) when heated above its glass transition (~100 °C). The Kapton tape (CAPLINQ, Ottawa Canada) had a thickness of 1 mil (0.025 mm). The Super Glue was purchased under the name of Loctite Liquid Professional Super Glue 20-Gram Bottle. Paperboard was cut from Staples colored file folder (red color in this experiment). The samples were placed in an oven (150 °C) for heating. Assembly typically finished in 2 min.

2.2. Pop-up by pushing from outside

The 2D precursor was fabricated by gluing red paperboard on a PS sheet (on both sides to make it symmetric). After the glue was fully cured, the paperboard/PS/paperboard sandwich became rigid and cannot shrink. A small gap (about 2 mm) was left between adjacent sandwich structures, i.e. bare PS strip without the paperboard. Since PS softens when heated, the gap acted as the soft crease during the buckling. The length of crease can be reduced to facilitate the folding. The PS sheets were perforated using a laser cutter.

2.3. Pop-up by pulling from inside

The 2D precursor was fabricated by connecting two panels of paperboard with a kapton tape. A small gap (about 2 mm) was left between the paperboard panels to make the soft crease. PS strips or sheets (of specific shape) were bonded onto the 2D precursor using Super Glue (with small gluing area, around 3 mm in size).

3. Results and discussion

3.1. Buckling induced by pushing from outside

First, we present buckling of 2D precursor that is pushed from outside. The 2D precursor was fabricated by modifying the polymer sheet locally (i.e. gluing rigid materials such as paperboard on both sides of the sheet). Folding along a single crease (i.e. uniaxial compression) is shown in figure 1. Within the polymer sheet (blue area) is the 2D precursor, which consists of two rigid panels (polymer sheet with paperboard bonded on both sides, in red) and a soft crease (polymer sheet only, in blue). In this case the 2D precursor can be viewed as a 1D structure (short in the transverse direction) inscribed in a narrow perforation in the polymer sheet, with the two ends anchored to and the two edges separated from the sheet by slits, respectively. As the polymer sheet shrinks, the perforation shrinks too with the same shrinkage ratio, causing buckling of the 1D structure. The buckling is concentrated at the crease due to its low stiffness while the rigid panels remain flat, forming a sharp angle. Note that the rigid panels rotate about the anchoring lines during the buckling. Based on the geometric relationship shown in figure 1(a), the folding angle can be calculated by

$$\cos(\alpha) = \frac{1 + \lambda^2 - [\zeta(1 + \lambda)]^2}{2\lambda} \tag{1}$$

where λ is the ratio between lengths of the two segments, ζ is the shrinkage ratio of the polymer sheet. The calculated and measured folding angles are plotted in figure 1(b) as functions of λ, where an equi-biaxially pre-strained polystyrene (PS) sheet was used as the actuation material, which shrinks to 46% of its initial length upon heating ($\zeta = 46\%$). The largest angle (55 degree) was obtained under the symmetric condition, i.e. $\lambda = 1$. The folding angle decreased with the increasing λ, until 0 degree at $\lambda = 2.7$. Note that equation (1) was not applicable when $\lambda > 2.7$, in which case the perforation shrank to $\lambda - 1$ in length (the minimum distance allowed by the two rigid panels), instead of $\zeta(1 + \lambda)$ (the distance obtained when PS fully shrinks to ζ). In other words, the shrinkage of the PS sheet/perforation was constrained by the rigid panels. The folding angle remained at 0 degree when λ was larger than 2.7.

The above is a special case with a 1D precursor. In general the 2D precursor is inscribed in a 2D perforation of a specific shape in the polymer sheet with its boundaries anchored to the sheet. The shrinkage of the polymer sheet causes the 2D precursor to buckle into a 3D structure. An example of this 2D-to-3D transformation is shown in figure 2. Here the 2D precursor includes a square panel surrounded by four rectangular panels (all rigid, red areas) and four soft creases (blue lines). The length of the creases (δ in figure 2(a)) can be reduced to facilitate the folding. As shown in

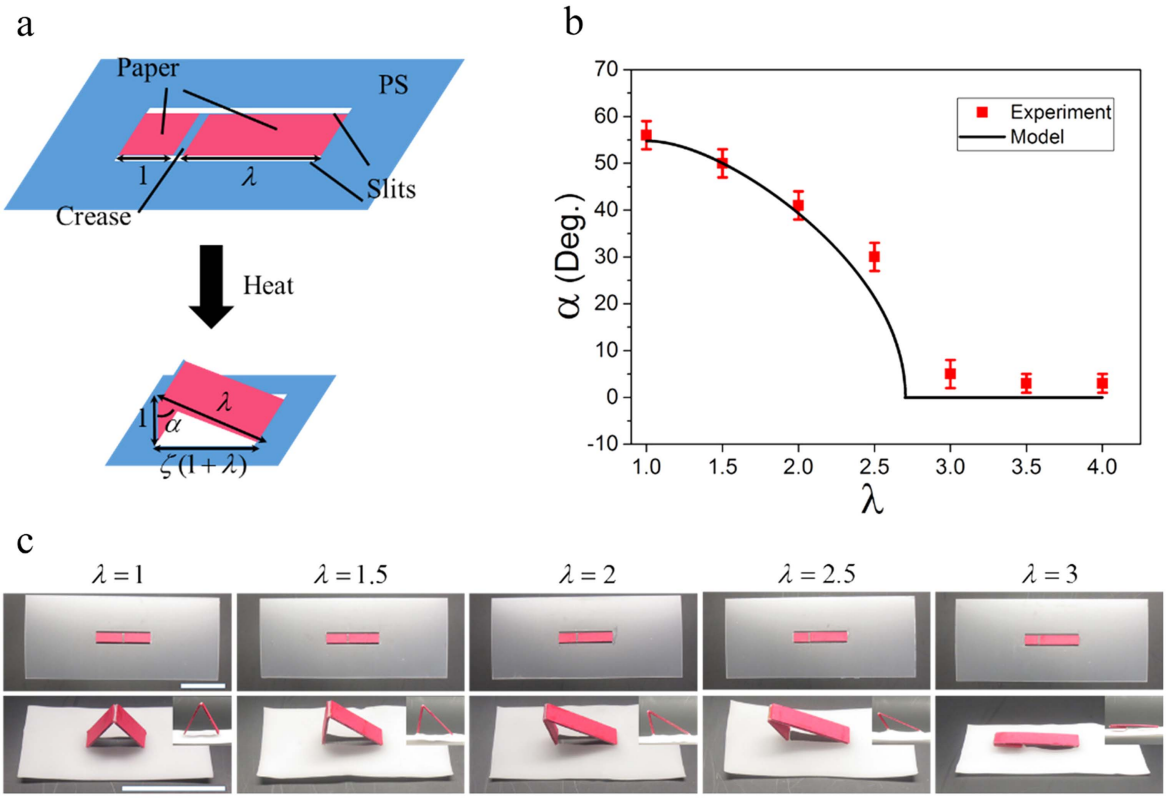

Figure 1. Folding along a single crease via the first approach. (a) Schematic of the folding process and geometric parameters; (b) Relationship between folding angle (α) and length ratio (λ); (c) Images of folding results at different length ratios (λ). Scale bars: 50 mm.

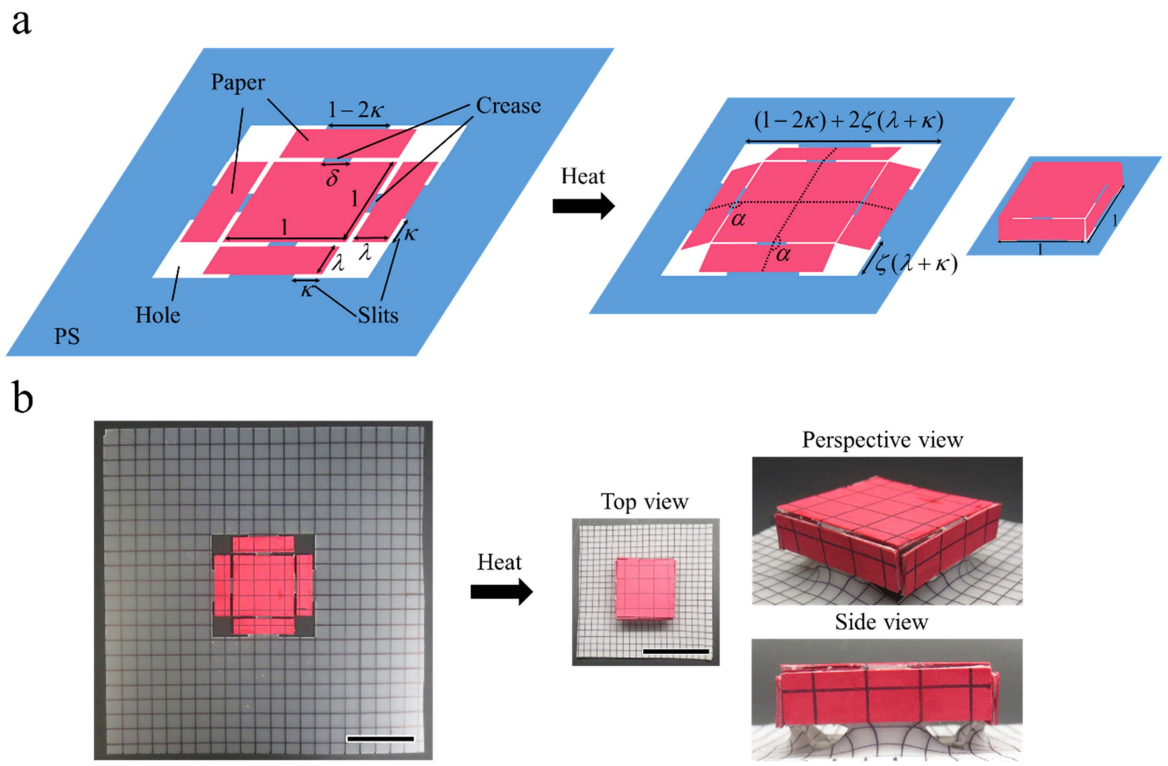

Figure 2. Assembling a square prism from its 2D precursor (first approach). (a) Schematic of the buckling process and geometric parameters. (b) Experimental realization of a square prism. Black gridlines were drawn to track the deformation. Scale bars: 30 mm.

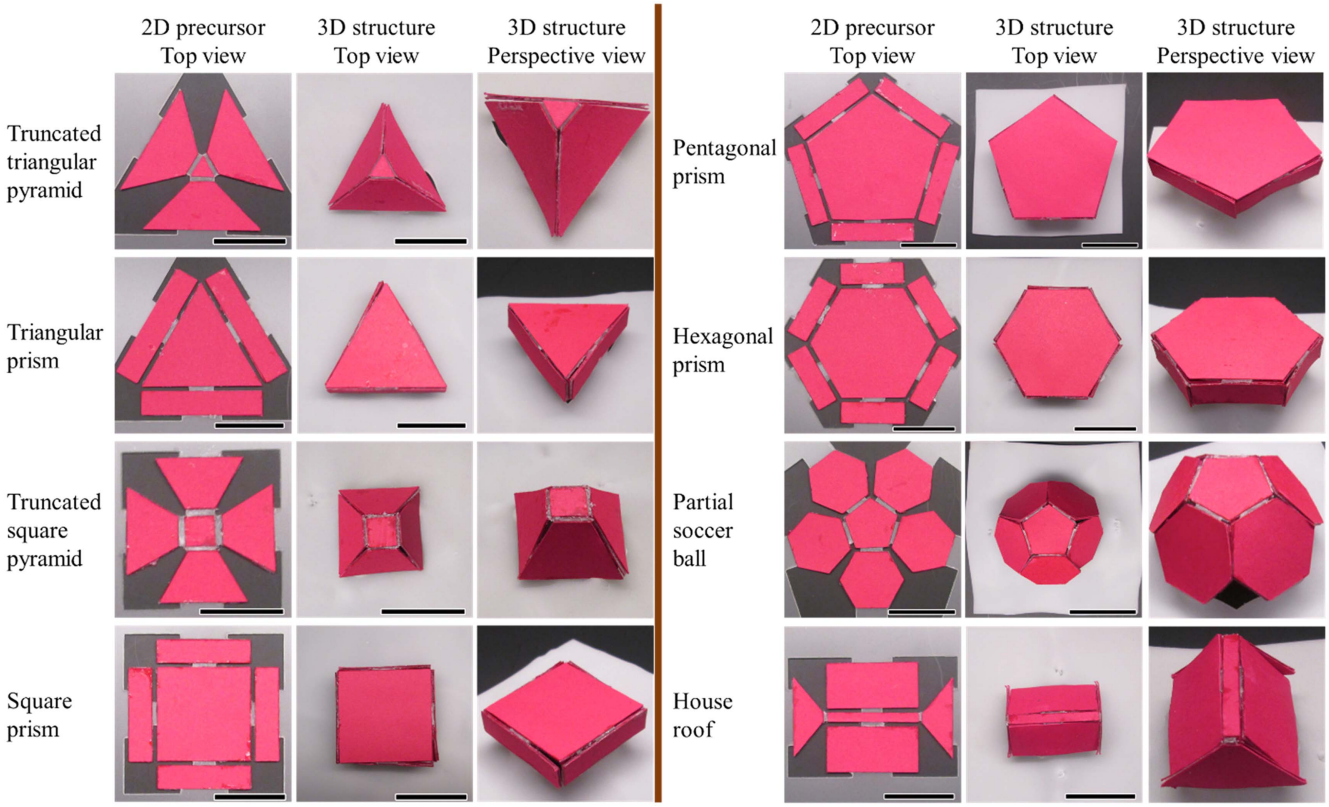

Figure 3. A number of 3D structures assembled via the first approach. Scale bars: 30 mm.

figure 2(a), four sides shrink in a symmetric manner, thus the square shape is retained. Slits (κ) are introduced in the anchoring lines to tailor the size of the perforation after shrinking, which determines the size of the final 3D structure. Initially (in the flat state), the square perforation has side length of $1 + 2\lambda$. As shown in figure 2(a), it shrinks to $(1 - 2\kappa) + 2\zeta(\lambda + \kappa)$ upon heating; the side length after shrinking decreases with increasing κ. Note that the portion anchored to the polymer sheet cannot shrink. The folding angle at the creases can be calculated by

$$1 - 2\lambda\cos(\alpha) = (1 - 2\kappa) + 2\zeta(\lambda + \kappa) \quad (2)$$

In order to get a right square prism ($\alpha = 90°$), the side of the perforation needs to shrink to 1, which means

$$(1 - 2\kappa) + 2\zeta(\lambda + \kappa) = 1 \quad (3)$$

Figure 2(b) shows the experimental realization of a square prism using a PS sheet. In order to monitor the deformation during the shrinking and buckling, black gridlines were drawn on the PS sheet and PS/paperboard panels before heating. The PS/paperboard panels were constrained from shrinking, as the black lines remained straight. The shrinkage was locally disturbed by the rigid PS/paperboard panels, which can be seen in the side view in figure 2(b) and more clearly when the slit length is reduced to zero. As shown in figure S1 is available online at stacks.iop.org/SMS/26/125011/mmedia, ESI†, without the slit, the size of the perforation after shrinking was larger than 1, which resulted in an open structure, instead of a closed prism.

This approach can be used to assemble prismatic and (truncated) pyramidal structures with different base shapes. Note that the in-plane shrinkage of the polymer sheet is isotropic and homogeneous, regardless of the perforation patterns. During shrinking, the perforation reduces its size while retaining its shape, which is different from the case when the equi-biaxial prestrain is applied mechanically (figure S2, ESI†). A number of 3D structures are presented in figure 3, including triangular prism/pyramid, square prism/pyramid, pentagonal prism and hexagonal prism. To assemble a 2D precursor into a closed prismatic/pyramidal structure, the perforation needs to shrink to the size of the base of the prism/pyramid. A partial soccer ball consisting of one pentagon and five hexagons was assembled with a pentagonal base. This approach can go beyond folding axisymmetric structures, i.e. regular polygon (equal angles/side lengths) based structures shown above. A house roof with a rectangular base was assembled as an example, where the 2D precursor is composed of two rectangles and two triangles surrounding a narrow strip. The 2D precursor is positioned in a rectangular perforation in the PS sheet. After shrinking, the size of the perforation is identical with the base of the house roof. Detailed calculations for each structure are given in figures S3 and S4, ESI†.

Figure 4 shows two special types of origami structures that can be folded using the above approach, each consisting of four rigid panels connected by four soft creases. These structures have only one degree of freedom, thus can be activated by uniaxial actuation. Figure 4(a) shows the Miura-ori structure,

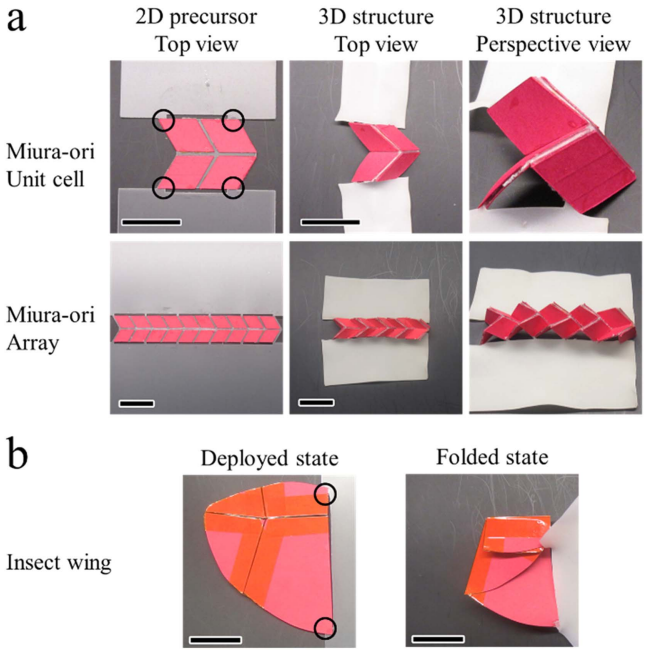

Figure 4. Origami with one degree of freedom. (a) Miura-ori and (b) Insect wing. Scale bars: 30 mm. The 2D precursor is bonded to the polymer sheet at discrete points (highlighted by black circles) with a slit between two points.

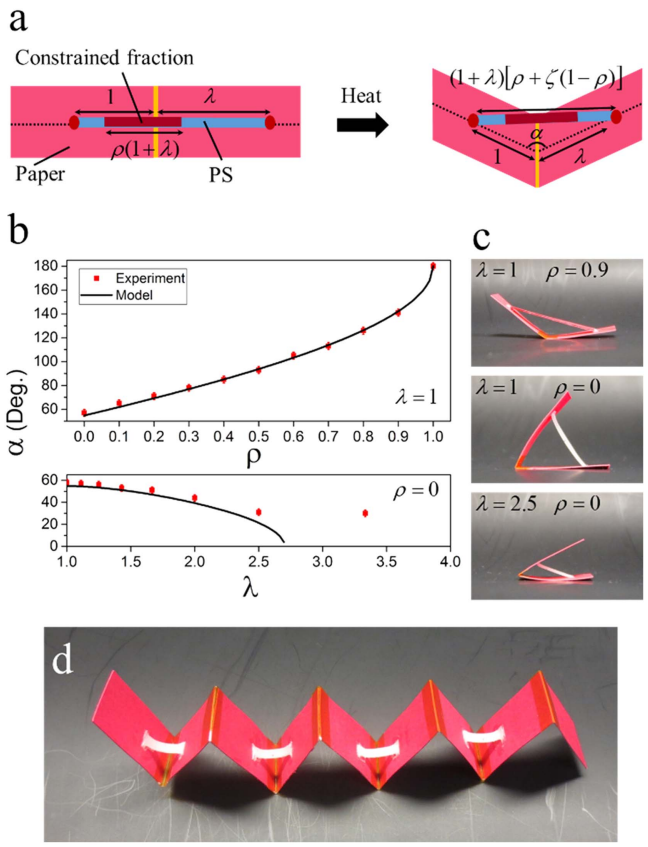

Figure 5. Folding a single crease via the second approach. (a) Schematic of the buckling process and geometric parameters; (b) Relationship between folding angle and length ratio (λ)/constrained fraction (ρ) for two special conditions; (c) Several folded samples; (d) A wavy structure.

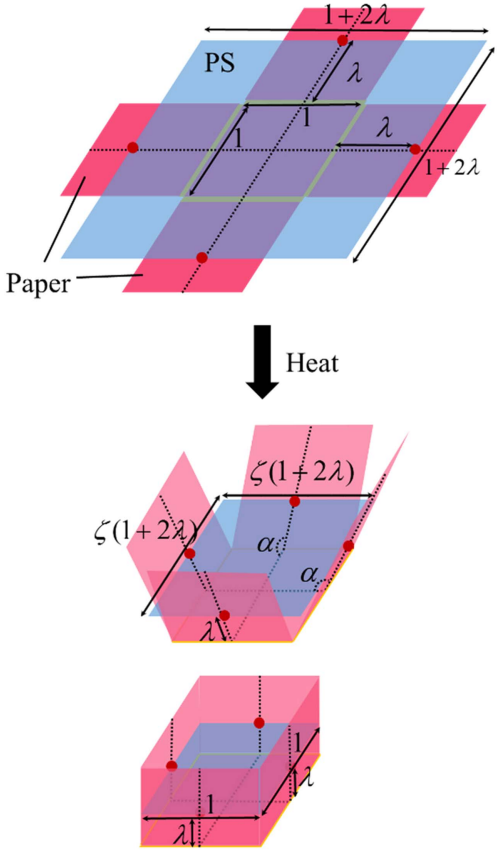

Figure 6. Assembling a square prism from its 2D precursor (second approach). Schematic of the buckling process and geometric parameters.

originally proposed by Miura as a method of packaging large membranes [10, 35]. Even though folding involves size reduction in both horizontal and vertical directions and pop-up out of plane, it can be activated solely by shrinking in the horizontal direction. This structure provides an excellent example of converting one-dimensional deformation into all three dimensions. Figure 4(b) shows another type of structure mimicking an insect wing [36]. When at rest, some insects (e.g. beetles) need to fold their delicate hindwings and tuck them under the protective forewings. The folding needs to be actuated by the basal muscles, since there are no muscles inside the wing. In other words, the actuation mechanism can be only connected to the structure (wing) on one side. This example illustrates that our approach can achieve 3D folding of a structure by contraction of a base on one side of the structure.

The approach shown above shares some characteristics with the compressive buckling reported previously [31]. While both are relatively simple and can be applied to fold many complicated structures, they have some limitations. For example, a large piece of polymer sheet (much larger than 2D precursor) is required. In addition, the assembled structure is always bounded by a polymer sheet, which may not be desirable for some applications.

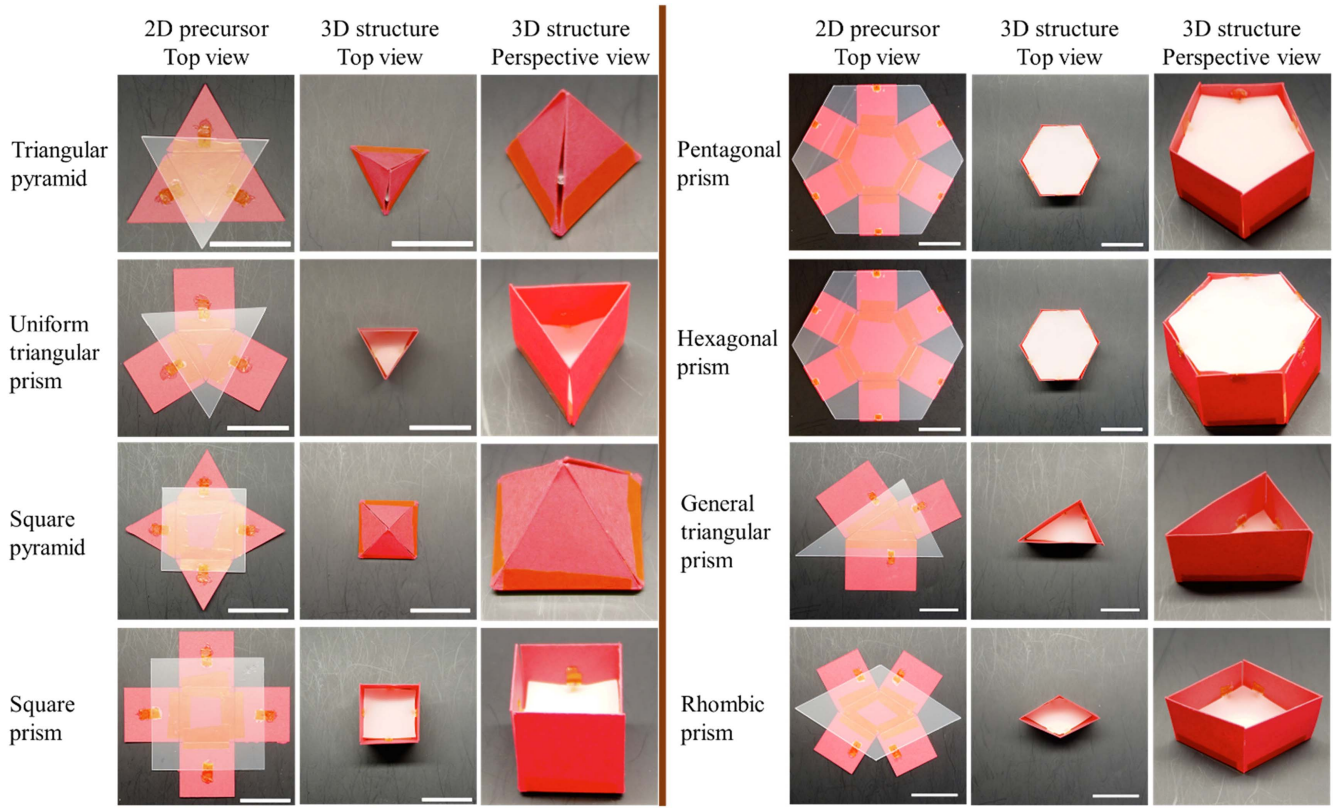

Figure 7. A number of 3D structures assembled via the second approach. Scale bars: 30 mm.

3.2. Buckling induced by pulling from inside

In order to circumvent such limitations, we developed another approach, where the polymer sheet pulls the 2D precursor from inside instead of pushing from outside. Figure 5 shows folding of a single crease using this approach as a starting case. Here the 2D precursor consists of two pieces of rigid paperboard connected with a soft crease (e.g. a strip of kapton tape). Note that here the rigid structure is the paperboard only, instead of the paperboard/polymer/paperboard sandwich in the first approach. A heat shrinkable polymer strip is placed on top of the 2D precursor, with two ends glued to two paperboard panels. The polymer strip shrinks upon heating, pulling the two paperboard panels toward each other and causing buckling. Again the buckling deformation is concentrated at the crease due to its low stiffness. Note that here λ is defined as the ratio of the two distances between the two bonding positions and the crease (figure 5(a)). In this approach, shrinkage of the polymer strip can be further controlled by constraining a certain fraction of it (e.g. by gluing rigid paperboard on both sides of the polymer sheet). The constrained fraction cannot shrink, while the rest of the polymer strip can shrink freely to ζ. As shown in figure 5(a), the folding angle is governed by

$$\cos(\alpha) = \frac{1 + \lambda^2 - \{(1 + \lambda)[\rho + \zeta(1 - \rho)]\}^2}{2\lambda} \qquad (4)$$

where ρ is the fraction of the polymer strip that is constrained from shrinking. Here we show two special cases to tailor the folding angle. The first case is to fix ρ at 0 and vary λ. The relationship between folding angle and λ is shown in the bottom panel of figure 5(b). Angles from 0 to 55 degrees can be obtained in theory. But practically angles smaller than 30 degree are difficult to achieve due to accumulation of the shrunk polymer strip inside the crease (as can be seen from the deviation of experimental results from the model at large λ). The second way is to fix λ at 1 and vary ρ. The relationship between folding angle and ρ is shown in the top panel of figure 5(b). Angles from 55 to 180 degrees can be obtained. PS was used again as the actuating polymer with $\zeta = 46\%$. Figure 5(c) shows several folded structures with different angles. Figure 5(d) shows a wavy structure by folding a chain of paperboard in alternated directions. According to equation (4), the folding angle is determined by the length ratio λ and the constraining fraction ρ, while the total length of the PS strip does not come into play here. This makes possible reducing the length of the PS strip without changing the folding angle. In the extreme condition that the PS strip is very short, it basically works as a hinge to cause folding of the 2D precursor, which is similar to the first strategy with responsive hinges as discussed in the Introduction [1, 21, 22].

Next, this approach is generalized to folding 2D precursor into 3D structures. Figure 6 shows the schematic of assembling a square prism from its 2D precursor as an example. The geometric rules are similar to those shown in figure 2(a). The bonding areas between the paperboard and the polymer sheet are very small (marked as the red dots in

figure 6) and can be regarded as points. This corresponds to $(1 - 2\kappa) = 0$ as shown in figure 2(a), where $1 - 2\kappa$ is the length of the anchoring line. In other words, there is no constraint on edges of the polymer sheet, thus the entire polymer sheet can shrink to ζ. The shape of 3D structure is determined by the size of the shrunk polymer sheet. The folding angle at the creases can be calculated by substituting $\kappa = 0.5$ in equation (2), which becomes

$$1 - 2\lambda \cos(\alpha) = \zeta(1 + 2\lambda) \tag{5}$$

Polymer sheets of different sizes $(1 + 2\lambda)$ can lead to different folding angles. In order to get a right square prism ($\alpha = 90°$), the shrunk polymer sheet needs to be identical in size with the base of the prism (1×1), which means

$$\zeta(1 + 2\lambda) = 1 \tag{6}$$

Figure 7 shows a set of 3D structures assembled using this approach, including uniform triangular prism/pyramid, square prism/pyramid, pentagonal prism, hexagonal prism, general triangular prism and rhombic prism. All structures were folded by PS sheets upon heating. The geometric calculations are the same as those for the truncated pyramids using the first approach as given in figures S3 and S4, ESI†. Three features distinguish this approach from the first approach discussed above and the one reported in literature [31]. First, the shrunk polymer sheet is within the 3D structure, instead of supporting it from underneath and/or surrounding it, which often times could be conducive to better appearances. Second, the panels of the 2D precursor can go beyond the bonding points, which allow increasing the height of the 3D structure and even form an enclosed structure while keeping the same base. For example, enclosed pyramids can be assembled using this approach (with a shrunk PS sheet inside). Third, the isolated 3D structures folded in this approach are easier to be tessellated or stacked to make more complex structures, as discussed in the following.

The prisms/pyramids shown in figure 7 can be tessellated side by side to make cellular structures. Figure 8(a) shows some examples of the cellular structures. Depending on the position of the PS sheet (i.e. above or below the 2D precursor), the 2D precursor can buckle upward or downward, which results in an array of prisms facing in alternated directions, resembling the checkboard pattern.

Another way to combine the prismatic/pyramidal structures is to stack them vertically, as shown in figure 8(b) [32]. Two square pyramids were combined (base to base) to make an octahedron, which consisted of 8 equal lateral triangles. Another example is a paperboard animal model. Multiple (truncated) hexagonal pyramids were stacked in the vertical direction, resulting in a paperboard animal. Both head and body were made of two (truncated) hexagonal pyramids facing each other. Both structures shown in figure 8(b) were popped up from multilayer 2D precursors, i.e. multiple 2D precursors stacked in the vertical direction.

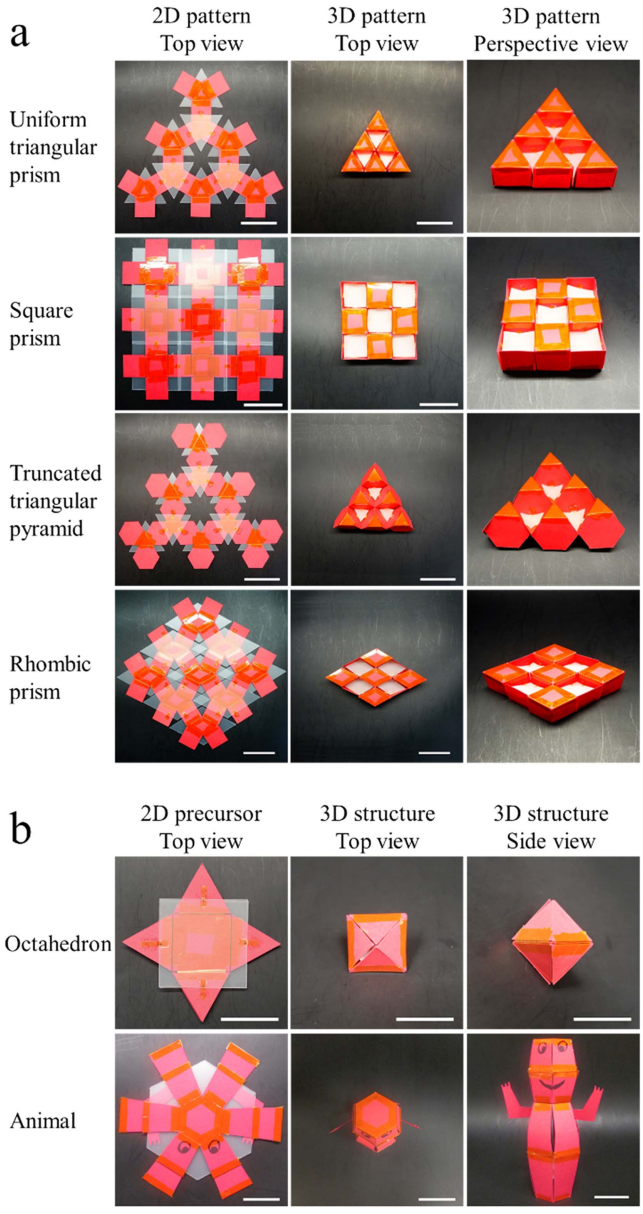

Figure 8. Combination of prismatic/pyramidal structures. (a) Horizontal tessellation (scale bars: 50 mm); (b) Vertical stack (scale bars: 30 mm).

3.3. Application of the cellular structures

Cellular structures can find applications in many fields, including packaging, energy absorbing and thermal insulating [37]. We used tessellation of the square prisms to demonstrate the thermal insulating property (figure 9). The assembled structure was sandwiched between two pieces of paperboard and placed on a hot plate. IR camera (model FLIR A655sc, FLIR Systems) was used to measure the temperature distribution. Another structure with three layers of paperboard was also placed on the hot plate for comparison. Black tapes (with emissivity ~0.95) were put on the hot plate and tested structures for the IR temperature measurement. Temperature of the hot plate was set to 150 °C. At thermal equilibrium, temperatures of the sandwich structure and the comparison structure were 51 and 118 °C, with the

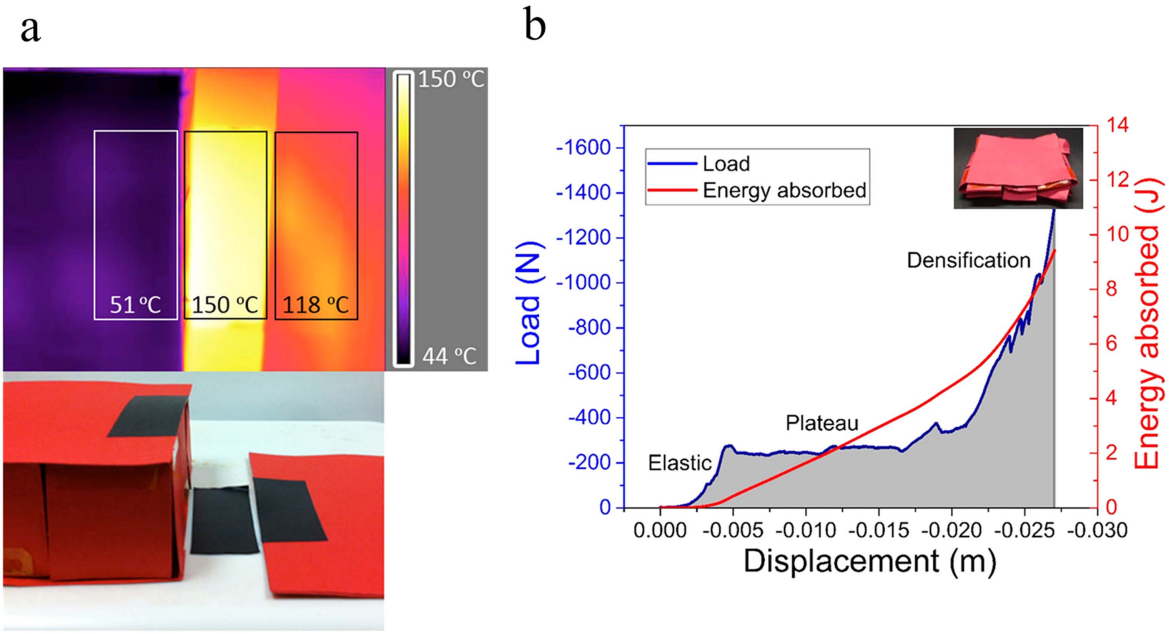

Figure 9. Application of cellular structure. (a) Thermal insulator; (b) Crash energy absorber.

corresponding heat transfer coefficient calculated to be 2.6 and 29.1 $Wm^{-2}K^{-1}$, respectively (Assuming heat transfer coefficient of air to be 10 $Wm^{-2}K^{-1}$ and ambient temperature as 25 °C). By assembling paperboard into cellular structures with enclosed air, the heat transfer coefficient was reduced by more than an order of magnitude.

The energy absorbing ability of the same structure was tested under compression. The cellular structure was about 25 g in weight, 90 mm × 90 mm in the horizontal plane and 30 mm in height. It was able to sustain 260 N compressive force before being crushed, corresponding to a nominal compressive stress of 32.1 KPa. The load-displacement curve shown in figure 9(b) consists of three stages. The displacement increases with the load initially (elastic stage) and then increases at a constant load (plateau stage) before the load increases rapidly (densification stage). The large deformation at the plateau stage contributes largely to the energy absorption. The energy absorbed in this case was 9.5 J (integrated area under load displacement curve) with the energy absorption per unit volume as 39 KJ m^{-3}. This is smaller than the reported value for paper honeycomb structures (50 KJ m^{-3}) [38]. The difference might be caused by the fact that in our structure, the vertical panels are separated from each other, thus deforms independently. While in the honeycomb structure, vertical panels are bonded together, thus the deformation are coupled together and requires more energy.

4. Conclusion

We have demonstrated self-assembly of complex 3D structures from their 2D precursors, actuated by a heat shrinkable polymer sheet. When heated, the polymer sheet shrinks in plane and causes the 2D precursor to buckle. The buckling is guided by the pre-defined creases in the 2D precursor due to their low stiffness. An equi-biaxially pre-strained PS sheet was used in this work as the actuation material. Two approaches were employed to achieve the assembly. In the first approach, the 2D precursor was inscribed in a perforation in the polymer sheet and pushed from outside upon heating. After transformation, a 3D structure inscribed in the shrunk perforation can be obtained. Assembled 3D structures included prisms/pyramids with different base shapes, partial soccer ball, house roof, Miura-ori structure and insect wing. In the second approach, the polymer sheet was placed on top of the 2D precursor, thus pulled it from inside. After transformation, the shrunk polymer sheet was enclosed within the 3D structure. Prisms/pyramids with bases of different shapes were assembled. The prisms can be tessellated to create cellular structures, which exhibited good thermal insulating and energy absorbing ability. They can also be stacked vertically to make multilayer complex structures. The geometric rules developed in this work are independent of length scale.

Acknowledgments

The authors acknowledge financial support from the National Science Foundation (NSF) through Award No. EFRI-1240438. The authors would like to thank Prof. M. D. Dickey for providing access to the laser cutter in his lab.

ORCID iDs

Jianxun Cui https://orcid.org/0000-0001-8286-490X

References

[1] Felton S, Tolley M, Demaine E, Rus D and Wood R 2014 A method for building self-folding machines *Science* **345** 644–6

[2] Hawkes E, An B, Benbernou N, Tanaka H, Kim S, Demaine E, Rus D and Wood R 2010 Programmable matter by folding *Proc. Natl Acad. Sci. USA* **107** 12441–5

[3] Leong T G, Randall C L, Benson B R, Bassik N, Stern G M and Gracias D H 2009 Tetherless thermobiochemically actuated microgrippers *Proc. Natl Acad. Sci. USA* **106** 703–8

[4] Song Z *et al* 2014 Origami lithium-ion batteries *Nat. Commun.* **5** 3140

[5] Cheng Q, Song Z, Ma T, Smith B B, Tang R, Yu H, Jiang H and Chan C K 2013 Folding paper-based lithium-ion batteries for higher areal energy densities *Nano Lett.* **13** 4969–74

[6] Fernandes R and Gracias D H 2012 Self-folding polymeric containers for encapsulation and delivery of drugs *Adv. Drug. Deliv. Rev.* **64** 1579–89

[7] Guan J, He H, Lee L J and Hansford D J 2007 Fabrication of particulate Reservoir-Containing, capsulelike, and Self-Folding polymer microstructures for drug delivery *Small* **3** 412–8

[8] Filipov E T, Tachi T and Paulino G H 2015 Origami tubes assembled into stiff, yet reconfigurable structures and metamaterials *Proc. Natl Acad. Sci. USA* **112** 12321–6

[9] Silverberg J L, Evans A A, McLeod L, Hayward R C, Hull T, Santangelo C D and Cohen I 2014 Using origami design principles to fold reprogrammable mechanical metamaterials *Science* **345** 647–50

[10] Schenk M and Guest S D 2013 Geometry of Miura-folded metamaterials *Proc. Natl Acad. Sci. USA* **110** 3276–81

[11] Rogers J A, Huang Y, Schmidt O G and Gracias D H 2016 Origami mems and nems *MRS Bull.* **41** 123–9

[12] Guo X, Li H, Ahn B Y, Duoss E B, Hsia K J, Lewis J A and Nuzzo R G 2009 Two-and three-dimensional folding of thin film single-crystalline silicon for photovoltaic power applications *Proc. Natl Acad. Sci. USA* **106** 20149–54

[13] Peraza-Hernandez E A, Hartl D J, Malak R J Jr and Lagoudas D C 2014 Origami-inspired active structures: a synthesis and review *Smart Mater. Struct.* **23** 094001

[14] Rafsanjani A and Bertoldi K 2017 Buckling-induced kirigami *Phys. Rev. Lett.* **118** 084301

[15] Sussman D M, Cho Y, Castle T, Gong X, Jung E, Yang S and Kamien R D 2015 Algorithmic lattice kirigami: a route to pluripotent materials *Proc. Natl Acad. Sci. USA* **112** 7449–53

[16] Castle T, Cho Y, Gong X, Jung E, Sussman D M, Yang S and Kamien R D 2014 Making the cut: lattice kirigami rules *Phys. Rev. Lett.* **113** 245502

[17] Saito K, Pellegrino S and Nojima T 2014 Manufacture of arbitrary cross-section composite honeycomb cores based on origami techniques *J. Mech. Design.* **136** 051011

[18] Tang Y, Lin G, Yang S, Yi Y K, Kamien R D and Yin J 2017 Programmable kiri-kirigami metamaterials *Adv. Mater.* **29** 1604262

[19] Tibbits S 2012 Design to self-assembly *Architectural Design* **82** 68–73

[20] Liu Y, Genzer J and Dickey M D 2016 '2D or not 2D': shape-programming polymer sheets *Prog. Polym. Sci.* **52** 79–106

[21] Tolley M T, Felton S M, Miyashita S, Aukes D, Rus D and Wood R J 2014 Self-folding origami: shape memory composites activated by uniform heating *Smart Mater. Struct.* **23** 094006

[22] Felton S M, Tolley M T, Shin B, Onal C D, Demaine E D, Rus D and Wood R J 2013 Self-folding with shape memory composites *Soft Matter* **9** 7688–94

[23] Bassik N, Stern G M and Gracias D H 2009 Microassembly based on hands free origami with bidirectional curvature *Appl. Phys. Lett.* **95** 091901

[24] Cui J, Yao S, Huang Q, Adams J G and Zhu Y 2017 Controlling the self-folding of a polymer sheet using a local heater: the effect of the polymer–heater interface *Soft Matter* **13** 3863–70

[25] Na J H, Evans A A, Bae J, Chiappelli M C, Santangelo C D, Lang R J, Hull T C and Hayward R C 2015 Programming reversibly self-folding origami with micropatterned photo-crosslinkable polymer trilayers *Adv. Mater.* **27** 79–85

[26] Ryu J, D'Amato M, Cui X, Long K N, Jerry Qi H and Dunn M L 2012 Photo-origami—bending and folding polymers with light *Appl. Phys. Lett.* **100** 161908

[27] Liu Y, Shaw B, Dickey M D and Genzer J 2017 Sequential self-folding of polymer sheets *Science Advances* **3** e1602417

[28] Liu Y, Boyles J K, Genzer J and Dickey M D 2012 Self-folding of polymer sheets using local light absorption *Soft Matter* **8** 1764–9

[29] Zhang Q, Wommer J, O'Rourke C, Teitelman J, Tang Y, Robison J, Lin G and Yin J 2017 Origami and kirigami inspired self-folding for programming three-dimensional shape shifting of polymer sheets with light *Ext. Mech. Lett.* **11** 111–20

[30] Liu Y, Mailen R, Zhu Y, Dickey M D and Genzer J 2014 Simple geometric model to describe self-folding of polymer sheets *Phys. Rev.* E **89** 042601

[31] Yan Z *et al* 2016 Controlled mechanical buckling for origami-inspired construction of 3D microstructures in advanced materials *Adv. Funct. Mater.* **26** 2629–39

[32] Yan Z *et al* 2016 Mechanical assembly of complex, 3D mesostructures from releasable multilayers of advanced materials *Sci. Adv.* **2** e1601014

[33] Xu S *et al* 2015 Assembly of micro/nanomaterials into complex, three-dimensional architectures by compressive buckling *Science* **347** 154–9

[34] Zhang Y *et al* 2015 A mechanically driven form of Kirigami as a route to 3D mesostructures in micro/nanomembranes *Proc. Natl Acad. Sci. USA* **112** 11757–64

[35] Miura K 1985 Method of packaging and deployment of large membranes in space *Inst. Space Astronautical Rep.* **618** 1–9

[36] Haas F and Wootton R J 1996 Two basic mechanisms in insect wing folding *Proc. R. Soc. Lond. B Biol. Sci.* **263** 1651–8

[37] Gibson L J and Ashby M F 1997 *Cellular Solids: Structure and Properties* 2nd edn (Cambridge: Cambridge University Press)

[38] Wang D 2009 Impact behavior and energy absorption of paper honeycomb sandwich panels *Int. J. Impact Eng.* **36** 110–4